IOP Conf. Series: Materials Science and Engineering **775** (2020) 012152 doi:10.1088/1757-899X/775/1/012152

Overall stability of steel web-tapered frame members

G I Belyy[1] and V U Askinazi[2]

[1] Saint-Petersburg State University of Architecture and Civil Engineering, 4, Vtoraya Krasnoarmeiskaya str., Saint-Petersburg, 190005, Russia
[2] OOO Petrocast silica, pom. 13N, 37A, Sedova str., Saint-Petersburg, 192148, Russia

E-mail: office@erkon.ru, vladimir.askinazi@gmail.com

Abstract. The solution to the problem of fully nonlinear stability analysis of web-tapered I-shaped members is presented in the paper. In order to accelerate the analysis, an analytical-numerical approach was applied in the solution. Nonlinear stability analysis in the elastic range is carried out by the use of the analytical procedure (so-called "Member" procedure) which is based on the combination of the results of buckling and linear analyses. The growth of the plastic deformations is taken into account by adding extra displacements in the "Member" procedure. These displacements are determined numerically in the process of incremental loading (so-called "Section" procedure). The proposed approach allows the calculation of all displacements at each load step and the estimating of the member's overall stability capacity, rapidly (up to 20 times faster than using shell-FEM) and accurately enough. The overall stability calculation results, depending on the different variables (slenderness, load eccentricities and their ratios, rigidity variations) under different load cases, are given in the paper. The stability capacity comparison between tapered and prismatic members is presented. Also the comparison with existent experimental researches' results is provided in the paper.

1. Introduction

Steel frames with web-tapered members are widely used nowadays. Material (stiffness) distribution through the length of such members corresponds with the internal forces diagram from the main load combination. This makes it possible to reduce the consumption of steel by an average of 15 to 30% in comparison with the same structures composed of prismatic members. However, frames composed of web-tapered members haven't spread widely in Russia because of an absence of stability calculation requirements in national design codes [1]. Also it should be noted that all available investigations in this field do not allow us to create an engineering calculation approach in the form existing in the Russian codes. Therefore, an analytical-numerical approach for carrying out stability analysis is proposed in this paper. As completed prismatic members stability researches [2, 3] have shown, this approach allows the performing of the member's overall stability analysis in the elastoplastic range rapidly and reasonably accurately.

2. Member's computational model

Member's computational model has traditional boundary conditions at both ends: bending about the major and minor-axis is free, torsion is prevented but warping is unrestrained. To perform stability analysis of a particular member, first of all, it needs to be detached from the frame. Detaching (extraction) of the member from a plane frame is conducted by its out-of-plane effective length. To

carry out this extraction it is necessary to perform an in-plane non-linear elastic analysis of the frame (without torsion) from the main load combination. The aim of this analysis is to determine second-order bending moments $M_{x,0}$, $M_{x,L}$ and compressive force N at the ends of the member at any load level.

Further in the paper the lower indexes "*L*" or "*0*" will relate to the forces and geometric properties at the deep or at the shallow end of the member, correspondingly.

Figure 1 represents loading case for extracted from plane frame I-shaped web-tapered member: compressive force is applied with eccentricities about both axes $e_{y,0} = M_{y,0}/N$, $e_{y,L} = M_{y,L}/N$, $e_{x,0} = e_{x,L} = l_{ef,y}/750 + i_x^{mid}/20$. The latter imply all the imperfections which could occur during the fabrication and erection processes of the frame.

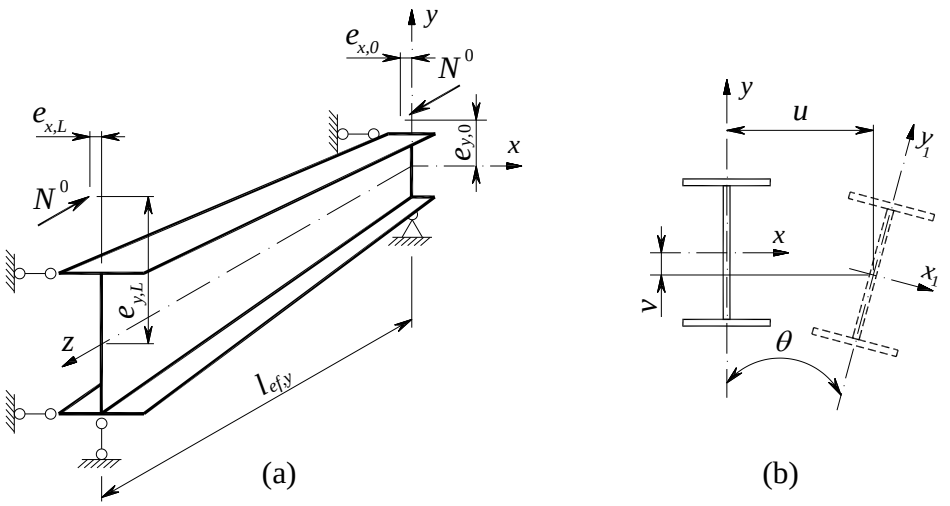

Figure 1. (a) – computational model; (b) – deflections of the member's cross-sections

3. Solution approach

The solution of the non-linear stability problem is based on the V.Z. Vlasov second-order theory of thin-walled members [4], extended by B.M. Broude [5] and E.A. Beilin [6] to the case when it is necessary to take into account the differences of the fibers' curvatures and the slopes associated with the torsion. In view of this fact the three differential equation system of equilibrium [6] (after the pre-integration of the first two) will be:

$$\begin{cases} EJ_x^* v'' + N^0 v - M_y^0 \theta + M_z^0 u' = -M_x^0 \\ EJ_y^* u'' + N^0 u + M_x^0 \theta - M_z^0 v' = -M_y^0 \\ \left[\dfrac{EJ_\omega^*}{\left(h_\omega^*\right)^2}\left(\theta h_\omega^*\right)''\right]'' h_\omega^* - \left[GJ_k^* \theta'\right]' - M_y^0 v'' + M_x^0 u'' + \left[i_p^{2^*} N^0 \theta'\right]' = 0, \end{cases} \quad (1)$$

where J_x^*, J_y^*, J_ω^* – bending and sectorial moments of inertia; J_k^* – torsional moment of inertia; h_ω^* – the distance between flanges' centroidal axes; all parameters marked " * " are variable through the length of the member; *v*, *u* – major- and minor-axis displacements, correspondingly; θ – the angle of torsion; *E*,*G* – Young's and shear moduluses, correspondingly; i_p – polar radius of inertia. Internal forces marked with index "0" are the results of the linear analysis of the member extracted from the plane frame.

There are some additional components in the third equation of the system (1) describing non-uniform torsion of the tapered members (because of the flanges' mutual incline). These components were first obtained by Cywinski and can be found in [7].

To solve the system (1) we use an analytical-numerical approach. By this approach the overall solution of the system (1) in elastic range can be presented as a combination of terms which can be obtained by executing separate analyses or calculations (so-called "Member" procedure) [8]:

$$v = v_l + v_b + v_a;\ u = u_l + u_b + u_a;\quad \theta = \theta_l + \theta_b + \theta_a. \tag{2}$$

The first terms in (2): v_l, u_l, θ_l – the linear deflections obtained by executing separate linear analyses of the member (when the influence of internal forces on the deflections is neglected) when only the "active" forces [9] are applied to the member:

$$\begin{gathered} EJ_x^* v_l'' = -M_x^0; \qquad EJ_y^* u_l'' = -M_y^0; \\ \left[\frac{EJ_\omega^*}{\left(h_\omega^*\right)^2}\left(\theta_l h_\omega^*\right)''\right]'' h_\omega^* - \left[GJ_k^* \theta_l'\right]' = 0;\ \left(B_\omega \neq 0\right). \end{gathered} \tag{3}$$

The solution of the equations (3) can be presented as:

$$v_l = V_l \psi_l(z);\quad u_l = U_l \varphi_l(z);\quad \theta_l = \Theta_l \nu_l(z), \tag{4}$$

where ψ_l, φ_l, ν_l – shapes of the deformed member; V_l, U_l, Θ_l – displacements' amplitudes which are linearly dependent of the "active" forces.

The second terms in (2): v_b, u_b, θ_b – the buckled shape functions obtained by executing the buckling analyses when only the "parametric" forces [9] are applied to the member. Equations for buckling analyses can be derived from the system (1):

$$EJ_x^* v_b'' + N^0 v_b = 0; \tag{5}$$

$$\begin{cases} EJ_y^* u_b'' + N^0 u_b + M_x^0 \theta_b = 0 \\ \left[\frac{EJ_\omega^*}{\left(h_\omega^*\right)^2}\left(\theta_b h_\omega^*\right)''\right]'' h_\omega^* - \left[GJ_k^* \theta_b'\right]' + M_x^0 u_b'' + \left[i_p^{2^*} N^0 \theta_b'\right]' = 0. \end{cases} \tag{6}$$

As one can see from (5) and (6), the system (1) has been divided into the buckling analysis of the centrally loaded member with the results of it represented in the similar way:

$$v_b = V_b \psi_b(z), \tag{7}$$

and the two equation system (6) of the lateral-torsional buckling of thin-walled member. After the execution of the latter we can obtain the lateral-torsional buckled shape functions:

$$u_b = U_b \varphi_b(z);\quad \theta_b = \Theta_b \nu_b(z). \tag{8}$$

In (7) and (8) V_b, U_b, Θ_b – some unknown constants having dimensions corresponding to v, u, θ (buckling analyses are executing with precision up to these constants); ψ_b, φ_b, ν_b – buckled shapes.

The third terms in (2): v_a, u_a, θ_a – the additional displacements about axes and the angle of torsion which can be caused by the spreading of the plastic deformations or possible local buckling or damages which reduce the cross-sections. Initial geometric imperfections can be applied in the solution by using these terms as well. They are approximated by algebraic or trigonometric polynomials and can be defined during incremental loading by determination of the equilibrium state for each cross section at each increment. It can be executed using so-called "Section" procedure [8] in

conjunction, for example, with the collocation method. According to the approach [8] after substituting (2) in the main system (1) the following can be obtained:

$$\begin{aligned} L_v &= EJ_x^* v_b'' + N^0 v - M_y^0 \theta + M_z^0 u' = 0; \\ L_u &= EJ_y^* u_b'' + N^0 u + M_x^0 \theta - M_z^0 v' = 0; \\ L_\theta &= \left[\frac{EJ_\omega^*}{\left(h_\omega^*\right)^2} \left(\theta_b h_\omega^*\right)'' \right]'' h_\omega^* - \left[GJ_k^* \theta_b' \right]' - M_y^0 v'' + M_x^0 u'' + \left[i_p^{2^*} N^0 \theta' \right]' = 0. \end{aligned} \tag{9}$$

From (9) it can be seen that they formally represent equations of equilibrium for a tapered member with initial geometric imperfections $v_l + v_a$, $u_l + u_a$, $\theta_l + \theta_a$ and which has received additional displacements caused by the action of the "parametric" forces [9].

Solve the system (9) by using energy stability criterion (Galerkin method):

$$\int_0^L L_v \psi_y''(z) dz = 0; \int_0^L L_u \varphi_y''(z) dz = 0; \int_0^L L_\theta \nu_y(z) dz = 0. \tag{10}$$

As a result we get the system of three algebraic equations for the unknown constants V_b, U_b, Θ_b of the buckled shape functions. After the solution of algebraic system, we will have all terms in (2) (v_a, u_a, θ_a – assumed to be defined, because they are determined using the "Section" procedure by achieving equilibrium states in all cross-sections at incremental loading process [8]). By using (2) we can obtain second-order internal forces:

$$\begin{aligned} M_x &= M_x^0 + N^0 v - M_y^0 \theta, \\ M_y &= M_y^0 + N^0 u + M_x^0 \theta, \\ B_\omega &= -\frac{EJ_\omega^*}{h_\omega^*} \left(\theta h_\omega\right)'' \end{aligned} \tag{11}$$

and stresses of any fiber of the cross-sections. At the same time the ultimate (failure) load (N^{ult}) for the "extracted" member is defined by the failure of its stable deformed state.

Returning to the general solution of (2), it should be noted that the complicated non-linear stability analysis was reduced to the buckling analysis. The latter could be executed numerically for each loading case.

The approach for determining the spatial displacements (u, v, θ) and the overall stability in elastoplastic range using the "Member" and the "Section" procedures is well described for prismatic members (for example [2, 3]) and here it was used the same. So let us pay attention on some results of the tapered members' stability analysis.

4. Stability analysis results

For the practical purposes, the results of the stability analyses are presented in the form of the stability factor $\varphi_{exy} = N^{ult} / R_y A_{mid}$ depending on: taper angle β_1, loading case, mid-length slenderness $\bar{\lambda}_y = \left(l_{ef,y} / i_x^{mid}\right) \sqrt{R_y / E}$ and non-dimensional eccentricity $m_{x,L}$ of compressive force N applied at the deep end. By then the stability check can be made in accordance with traditional formula existed in the Russian steel design codes [1]:

$$\frac{N}{\varphi_{exy} \gamma_c R_y A_{mid}} \le 1, \tag{12}$$

where A_{mid}, i_x^{mid} – mid-length cross-sectional area and radius of inertia, correspondingly; R_y – design yielding stress; γ_c – service factor.

3 loading cases were considered in the research (Figure 2).

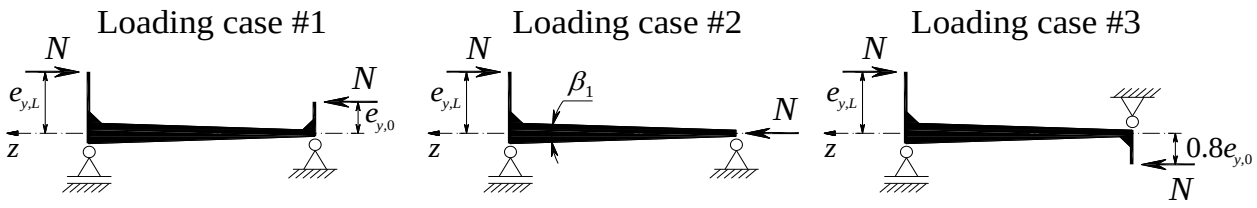

Figure 2. Loading cases

Absolute eccentricities at the shallow end $e_{y,0}$ were taken on the assumption of equal fiber stress at both ends:

$$e_{y,0} = \frac{e_{y,L} W_{x,0}}{W_{x,L}} + \left(\frac{1}{A_L} - \frac{1}{A_0} \right) W_{x,0} . \tag{13}$$

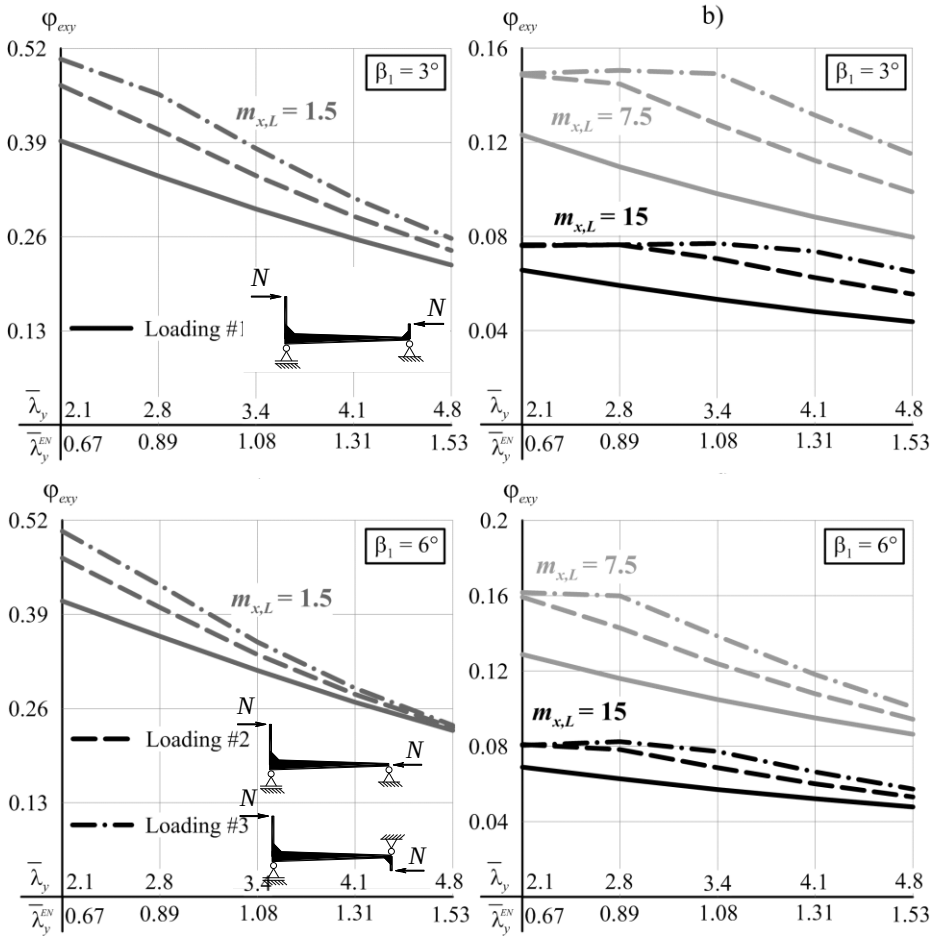

Figure 3. Overall stability analysis results: stability factors φ_{exy} at different slenderness

Graphs in Figure 3 represent the dependence of stability factors φ_{exy} (when $\beta_1 = 3°$ and $6°$) on slenderness $\bar{\lambda}_y$ ($\bar{\lambda}_y^{EN}$ – slenderness according [10]) at different eccentricities $m_{x,L}$ when $R_y = 24.5\ kN/cm^2$. Mid-length cross-sections of all the members were taken to be the same (with the relationship of radiuses of inertia $i_y^{mid}/i_x^{mid} = 4.4$) – thus the members of the same slenderness have equal weight.

The solid lines correspond to the one-sided end eccentricities (loading case #1), dashed lines – when there is $m_{x,0} = 0$ at the smaller end (loading case #2), dash-dot lines correspond to the case when the eccentricities are opposite in direction at the ends (loading case #3).

The graphs in Figure 3 reveal that when the eccentricities ($m_{x,L} = 1.5; 7.5; 15$) are equal, the load carrying capacity (φ_{exy}) is considerably higher for the loading cases #2 and #3 than for case #1. However, with a growth of slenderness these differences become less significant.

The graphs in Figure 4 demonstrate the dependence of stability factors φ_{exy} on the taper angle β_1 at the different slenderness and eccentricities $m_{x,L}$ when $R_y = 24.5\ kN/cm^2$. It is worth remembering that the members of the same slenderness have equal weight.

As can be seen from the graphs in Figure 4 the stability capacity at loading case #1 increases with the growth of taper angle, while at loading cases #2 and #3 the contrary occurs: it decreases and, moreover, in case #3 this trend is more pronounced. For members with relatively low slenderness at loading cases #2 and #3 when the eccentricities are high enough there can be found such a taper angle when the stability capacity reaches a peak (for example, for $\bar{\lambda}_y = 3.4$ at $m_{x,L}$=15 and the loading case #3 its β_1=4.5°).

The stability capacity comparison of tapered and prismatic members of equal weight is also carried out. For this purpose, prismatic members were loaded with the same eccentricities as tapered ones. It was obtained that for the most common taper angles (from 3° to 6°) the tapered members stability capacity is above prismatic ones on the average of 6.5%, 18.2% and 24.8% for loading case #1, #2 and #3, respectively.

5. Comparison with experimental researches

In order to verify the proposed approach, comparisons of the results of existent experimental researches with tapered members were carried out.

First comparison – with results of the experimental research made by Salter, Anderson and May (1980) [11], who conducted a series of tests with steel welded I-shaped tapered beam-columns. A total of 8 specimens were tested, including: C1 to C5 – specimens with no intermediate restraints, C6 and C7 – specimens which tension flange was held against lateral displacement, C8 – specimen whose compressed flange was restrained against lateral displacement.

Specimen C8 was excluded from the comparison due to its mid-length restraints, but specimens C6 and C7 were included because their restraints had no influence on the overall behavior of the members under load (it was pointed out by the authors [11]).

The stages of applying loads as well as the residual stress pattern in the proposed approach calculations were assumed the same as in the paper [11].

Comparison of the failure bending moments obtained by the proposed approach (M_{calc}) and in the experimental research (M_{exp}) is given in Table 1.

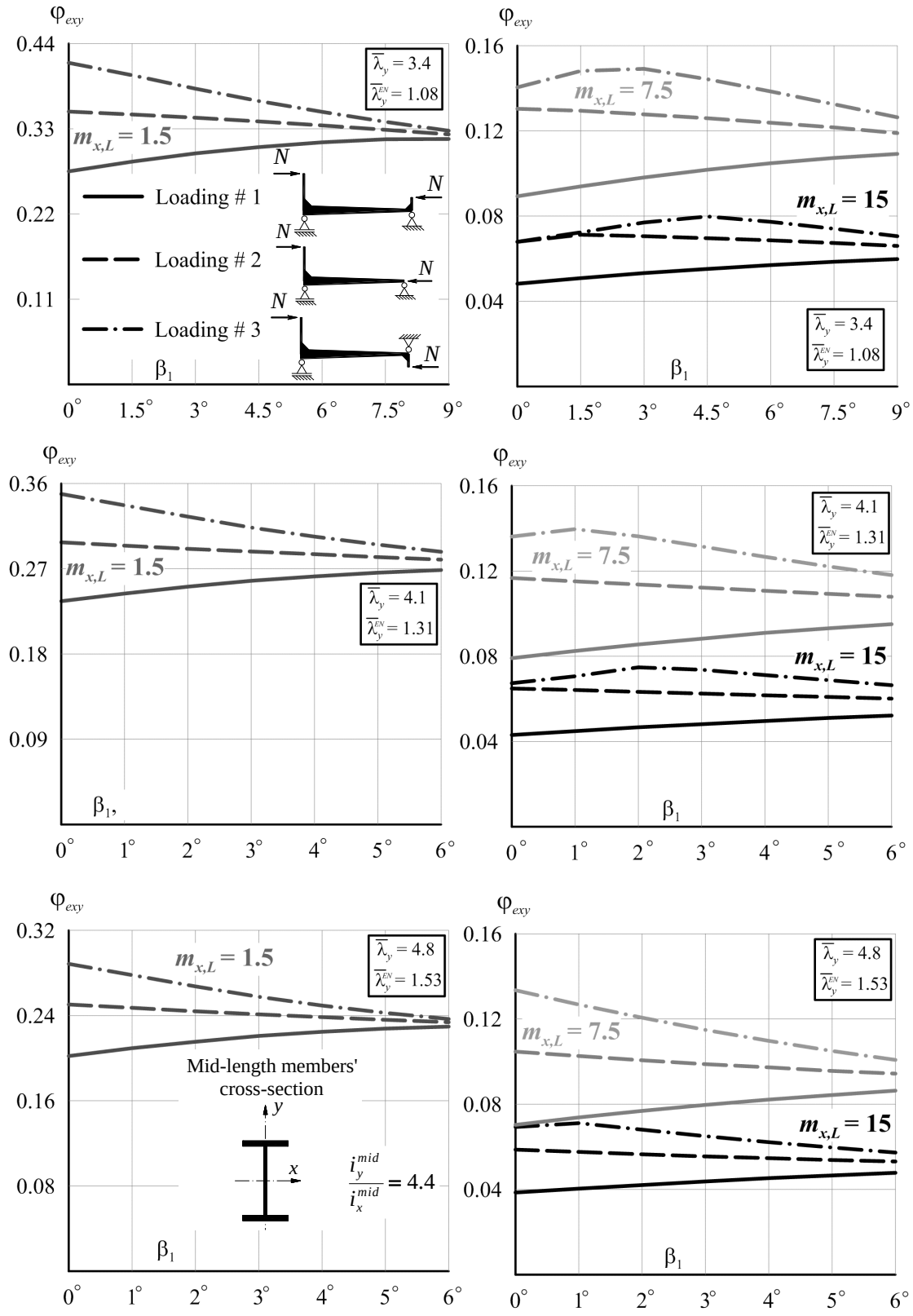

Figure 4. Overall stability analysis results: stability factors φ_{exy} at different taper angles

Table 1. Comparison between results obtained by the proposed approach and experimental tests [11]

Speci-men	Effective length L, mm	Taper angle β_1	Mid-length slenderness λ_y^{mid}	Yielding stress σ_y, kN/cm^2	Failure bending moments		Difference $\frac{M_{exp}-M_{calc}}{M_{exp}}\cdot 100\%$
					M_{exp}, kNm	M_{calc}, kNm	
C1	2622	4.2°	118	32.5	82.8	63.7	+23.1
C2	2620	3.7°	115	32.5	53.0	53.4	-0.8
C3	2619	3.1°	113	32.5	45.6	43.3	+5.0
C4	1903	5.3°	103	31.5	44.6	42.5	+4.7
C5	1903	3.6°	100	31.5	22.3	22.2	+0.4
C6	2619	3.7°	114	33.5	53.9	55.0	-2.0
C7	2619	3.1°	113	33.5	47.4	46.9	+1.1

It can be seen from Table 1 that the results of theoretical calculations by the proposed approach and experimental study are in a good agreement. In 85% of cases the difference did not exceed 5%, and only one case (specimen C1) was a 23.1% difference gotten. However, fully non-linear FEM stability analysis of the shell model in ABAQUS (which was carried out by Kim [12]) gave an even lower value of ultimate moment: 56.6 kNm. This fact may prove that the authors [11] could not have provided the right or the full initial data about this specimen or could have made a mistake in the value of the ultimate moment.

Figure 5 presents curves of major axis displacements (displacements "*v*") at mid-length for specimens C2 and C4. In addition, the curves obtained by the authors' numerical calculations [11] are also provided.

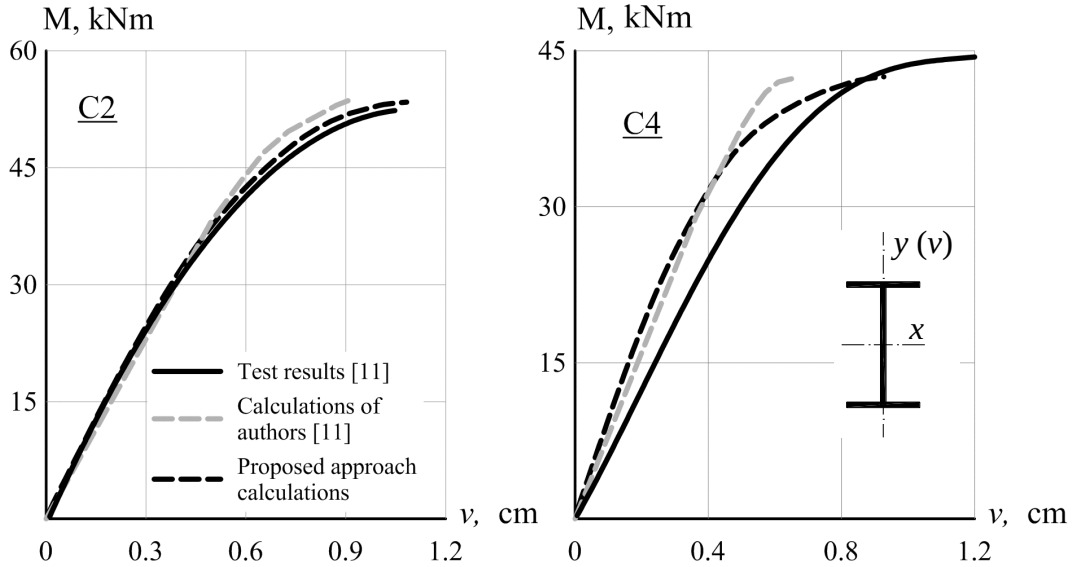

Figure 5. Major-axis displacements at mid-length for C2 and C4 specimens

As can be seen from the graphs in Figure 5 the curves obtained by the proposed approach are in a good agreement with the curves obtained from experimental data and the authors' numerical calculations [11].

Second comparison – with results of the experimental research made by Shiomi, Nishikawa and Kurata (1983) [13], who conducted three series of tests with tapered I-shaped beam-columns. The present comparison includes only the results of the OT-series test in which the specimens (19 items) were not held against lateral displacements and whose loss of stability occurred in the overall mode (involves two displacements *v*, *u* and the angle of torsion θ). Comparison of the failure loads obtained by the proposed approach (N_{calc}) and the experimental tests ($N_{\exp}$) is given in Table 2 from which it can be seen that in 63% of cases (12 specimens) the difference in ultimate (failure) loads did not exceed 5%. The highest differences +15% and -12.8% were obtained for specimens OT-1.6-1 and OT-1.6-2, respectively. Regarding OT-1.6-1: fully non-linear FEM stability analysis of the shell model in ABAQUS (which was carried out by Kim [12]) gave an average (for the three residual stress patterns) difference of +14.4% what may prove that the authors [13] did not provide complete data about this specimen initial imperfections. Regarding OT-1.6-2: when the test was conducting, the center compressive load position was accidentally shifted to out-of-plane direction [13], which in turn, created additional bending moments led to a failure at lower ultimate load.

Table 2. Comparison between results obtained by the proposed approach and experimental tests [13]

Specimen	Effective length L, mm	Mid-length slender-ness λ_y^{mid}	Taper angle β_1	Eccentri-city, $m_{x,L}$	Average yielding stress σ_y, kN/cm^2	Failure load		Difference $\frac{N_{\exp}-N_{calc}}{N_{calc}}\cdot 100\%$
						$N_{\exp}$, kN	N_{calc}, kN	
OT-1.4-2	2000	68	1.3°	1.69	30.27	370	349	+5.7
OT-1.4-4	2500	78	1.1°	2.47	28.64	252	250	+0.8
OT-1.6-1	3000	172	1.7°	8.02	29.39	80	68	+15.0
OT-1.6-2	2000	76	2.0°	1.04	29.90	358	404	-12.8
OT-1.6-4	2500	81	1.7°	1.50	29.88	361	373	-3.3
OT-1.6-5	3000	100	1.4°	2.39	30.30	247	259	-4.9
OT-1.8-1	2000	75	2.5°	1.02	29.56	412	413	-0.2
OT-1.8-3	2500	87	2.1°	1.49	29.86	357	350	+2.0
OT-1.8-4	2500	88	2.4°	2.55	30.59	265	271	-2.3
OT-1.8-5	3000	100	1.9°	2.32	29.70	259	272	-5.0
OT-2.0-1	2000	85	2.9°	0.92	30.17	356	358	-0.6
OT-2.0-3	2500	112	2.9°	2.45	29.99	225	235	-4.4
OT-2.0-4	3000	100	2.3°	2.47	29.75	293	285	+2.7
OT-2.0-5	3000	100	2.4°	1.51	29.83	402	377	+6.2
OT-2.2-3	2500	89	3.2°	1.54	29.65	351	349	+0.6
OT-2.2-5	3000	103	2.8°	2.58	30.03	279	251	+10.0
OT-2.4-1	2000	87	4.0°	0.93	30.34	406	382	+6.3
OT-2.4-3	2500	108	3.2°	1.38	30.26	287	287	0
OT-2.4-4	3000	102	3.3°	2.50	29.81	309	286	+7.4

Third comparison – with results of the experiment made by Cristutiu, Nunes and Dogariu (2012) [14], who also conducted three test series with tapered I-shaped beam-columns. The comparison includes only the results of the NR-series tests in which the specimens (2 items with the same dimensions differentiate in web thickness: 8 and 6 mm) did not have any intermediate restraints. The differences of 0.1% and -9.9% (Table 3) in failure bending moments were obtained for specimens C1_8_NR and C1_6_NR, respectively. Almost 10% difference for the latter is explained by the fact that the local buckling of the flange occurred first followed by the overall stability loss.

Table 3. Comparison between results obtained by the proposed approach and experimental tests [14]

Specimen	Effective length L, mm	Taper angle β_1	Mid-length slenderness λ_y^{mid}	Yielding stress, σ_y, kN/cm^2		Failure bending moments		Difference $\frac{M_{\exp} - M_{calc}}{M_{\exp}} \cdot 100\%$
				web	flanges	$M_{\exp}$, kNm	M_{calc}, kNm	
C1_8_NR	3600	5.6°	83.8	41.0	26.7	488.75	488.4	+0.1
C2_6_NR	3600	5.6°	79	31.9	26.7	395.75	434.8	- 9.9

Presented comparisons with the results of 3 experimental researches [11, 13, 14] confirm the validity and adequate accuracy of the proposed analytical-numerical approach for the carrying out fully non-linear stability calculations of tapered members.

6. Summary

Thus, the use of the proposed analytical-numerical approach (where the buckling shapes are determined numerically) affords to obtain new results of the tapered members' stability analyses with high speed (up to 20 times faster than carrying out the same analyses by shell-FEM) and adequate accuracy. These results can be widely use in structural steel design.

References

[1] Vedyakov I I et al 2017 *SP16.13330.2017: Steel Structures, Revised Edition SNiP II-23-81** (Moscow: Standartinform)
[2] Rodikov N N 1987 *Stability of Open Section Structural Members Under Biaxial Thrust* (Leningrad: Leningrad Civil Engineering Institute)
[3] Sotnikov N G 1987 *Strength and Stability of Angle Section Structural Members Having General and Local Defects and Damages* (Leningrad: Leningrad Civil Engineering Institute)
[4] Vlasov V Z 1959 *Thin-Walled Elastic Beams* (Moscow: Fizmatgiz)
[5] Broude B M 1959 *Research on Structural Theory* **8** 205-223
[6] Beilin E A 1969 *Structural Mechanics and Analysis of Constructions* **5** 35-41
[7] Cywinski Z 1969 *Rozprawy Inzynierskie* **17** 185-217
[8] Belyy G I 1987 *Spatial Behavior and Ultimate States of Metal Structural Members* (Leningrad: Leningrad Civil Engineering Institute)
[9] Rzhanitsin A R 1955 *Elastic Systems' Stability of Equilibrium* (Moscow: Gostehizdat)
[10] Denton S et al 2014 *EN-1993-1-1:2005, Eurocode 3: Design of steel structures, Part 1-1: General rules and rules for buildings* (Brussels: CEN)
[11] Salter J B, Anderson D and May I M 1980 *The Structural Engineer* **58A(6)** 189-193
[12] Kim Y D 2010 *Behavior and Design of Metal Building Frames Using General Prismatic and Web-tapered Steel I-section Members* (Atlanta: Georgia Institute of Technology)
[13] Shiomi K, Nishikawa S and Kurata M 1983 *Memoirs of Chubu Institution of Technology* **19-A** 55-66
[14] Cristutiu I M, Nunes D L and Dogariu A I 2012 *Int. J. Steel and Comp. Struct.* **13(3)** 225-238